ELSEVIER

International Journal of Solids and Structures 41 (2004) 3081–3094

INTERNATIONAL JOURNAL OF SOLIDS and STRUCTURES

www.elsevier.com/locate/ijsolstr

Seismic analysis of large 3-D underground caverns based on high performance recursive method

Jianyun Chen, Jing Li *, Jing Zhou

Construction Management Division, Institute of Engineering Earthquake Research, School of Civil and Hydraulic Engineering, Dalian University of Technology, Dalian 116023, China

Received 2 July 2003; received in revised form 7 January 2004

Available online 28 February 2004

Abstract

In the present paper, the seismic response of a large underground hydropower plant, which is located in southeast China, is investigated and a high performance recursive procedure based on the damping-solvent extraction method (DSE) is proposed for the study of the dynamic stiffness matrix of unbounded rock medium. An analytical formula for the derivative of the dynamic stiffness matrix of unbounded medium with respect to frequency is given, which can reduce the computational cost for a specified frequency. Then a recursive procedure is derived to converse the solving of the inverse matrix at a series of frequencies to step-by-step matrices multiplication, which can reduce the computational cost dramatically. The proposed procedure incorporated with substructure method is implemented in a finite element code for the dynamic analysis of a large three-dimensional underground hydropower plant caverns subjected to seismic excitation. Numerical tests on several representative unbounded domain wave problems demonstrate excellent accuracy and efficiency.

Keywords: Dynamic interaction; Unbounded medium; Seismic; Underground; Recursive; Impedance

1. Introduction

The seismic response analysis of underground structures is very complicated and difficult because of the unbounded medium–structure dynamic interaction and the uncertainty of earthquake excitation, especially for large scale underground caverns of hydroelectric power stations. The constraints and radiation damping of the unbounded medium have great effects on the seismic response of underground structures.

Required in the substructure method for the earthquake analysis of large three-dimensional underground caverns is the impedance matrix (or the frequency-dependant dynamic stiffness matrix) for the unbounded rock medium region, which is defined at the nodal points on the rock-structure interface. But the influence of the unbounded rock medium on underground structures is a difficult problem for the

* Corresponding author. Tel.: +86-411-4707541; fax: +86-411-4674141.
E-mail addresses: eerd001@dlut.edu.cn, lijng7402@sohu.com (J. Li).

0020-7683/$ - see front matter © 2004 Elsevier Ltd. All rights reserved.
doi:10.1016/j.ijsolstr.2004.01.023

dynamic rock-structure interaction analysis. Up to now, the computation of the impedance of unbounded medium has been the subject of many investigations over past years and a variety of analysis techniques are proposed, such as the frequency domain BEM used by Stamos and Beskos (1995), dynamic infinite element by Zhao and Valliappan (1993), periodic infinite solid element by Chow and Smith (1981), cloning method by Dasgupta (1982), transmitting boundary by Werkle (1987) and many other methods. The study by Wolf and his cooperators, including recursive method in time domain (Wolf and Motosaka, 1989), finite element multi-cell cloning method (Wolf and Song, 1994b), consistent infinitesimal finite-element cell method (Wolf and Song, 1994a), forecasting method (Wolf and Song, 1995), damping-solvent extraction method (Wolf and Song, 1996) etc., have helped to the development of comprehension of physical essence and computation methods on dynamic soil–structure interaction analysis. More general address on the dynamic analysis of underground structures can be found in the paper by Stamos and Beskos (1995). But few methods is widely accepted in engineering practice because of the complication and high computational cost induced by the determination of the dynamic stiffness matrix of the unbounded medium. Dependence on frequency leads to the determination of the dynamic stiffness matrix of the unbounded medium at a serial of discretized frequencies in frequency domain or the convolution integrals in time domain.

Among all these methods, the so-called damping-solvent extraction method (DSE), refined as discussed in this paper, can be easily accepted and implemented because of conceptual conciseness and programming simplicity. In addition, it is suitable to be applied to any complex geological or geographic conditions, such as the canyon rock condition in which located many high dams in south-west China, while some other methods have strict restrictions on element geometry or material composition that would cause some difficulties in application.

The purpose of this paper is to present a general, efficient numerical method to determine the dynamic response of the unbounded medium–structure system based on refined DSE Method.

Firstly, an analytical formula for the computation of the derivative of the dynamic stiffness matrix of unbounded medium with respect to frequency is suggested, which cost only one third computational efforts for a specified frequency of that by the difference method (Wolf and Song, 1996).

Then an iterative approach (or transfer matrix approach) is proposed for the inverse matrix evaluation. This is the key point for the whole refined procedure, which makes use of the property that the product of the reverse matrix of stiffness with the mass matrix is a very small quantity. By comparison with the direct method, the decomposition of the complex matrix is avoided which contributes a great to the computational cost.

And at last, a recursive procedure is put up for the determination of dynamic stiffness matrix of unbounded wall rock at a series of frequencies, which can start from any specific frequency of interested.

The numerical test and the application of the proposed procedure to large underground power plants is presented. The results show that the proposed procedure has better accuracy and lower cost in computing the dynamic stiffness of the wall rocks compared to existing methods, and in the current engineering design practice of underground structures in seismic active area, the present method can greatly simplify computation and improve the efficiency.

2. Impedance of unbounded medium

In the substructure method for the unbounded medium–structure dynamic interaction analysis, the effect of the unbounded medium on the underground structures can be expressed as the interaction force acted on the unbounded medium–structure interface. In the frequency domain it can be expressed as (Wolf and Song, 1996)

$$\boldsymbol{R}(\omega) = \boldsymbol{S}^{\infty}(\omega) \cdot \boldsymbol{u}(\omega) \tag{1}$$

In which $\boldsymbol{R}$ is the interaction force on the unbounded medium–structure interface, $\boldsymbol{u}$ is the displacement in the nodes on the interface, $\boldsymbol{S}^{\infty}(\omega)$ is the frequency-dependent dynamic stiffness matrix of the unbounded medium.

There are many approaches for the determination of the infinite domain impedance, several methods have been tried, including infinitesimal cell method, boundary element, dynamic infinite element and transmitting boundary method, and finally the damping-solvent extraction method is employed, although the computational cost of it is not less than that of other methods, the concept is concise and the implementation is very easy.

2.1. Concept of damping-solvent extraction method

The damping-solvent extraction method consists of three steps (Wolf and Song, 1996). In the first step, the unbounded medium is truncated by an artificial boundary and an artificial damping which is not present in the actual medium is introduced as solvent. The effect of this damping includes reducing the amplitudes of the outgoing waves propagating from the structure–medium interface towards the outer boundary and after reflection diminishing the amplitudes of the reflected waves to negligible amplitudes when reaching the structure–medium interface. Thus the structure–medium interface's motion depends only on the outgoing waves. All the degrees of freedom of this bounded medium with the exception of those on the structure–medium interface can be eliminated, leading to the dynamic-stiffness matrix of the damped bounded medium. In the second step, the dynamic stiffness matrices obtained in the first step is assumed to be equal to the corresponding values of the damped unbounded medium as no reflected waves existed at the structure–medium interface. In the third step, the influence of the introduced artificial damping on the dynamic stiffness matrix is extracted to obtain the dynamic stiffness matrix of the un-damped unbounded medium. The computational efforts of extraction can be neglected compared with that of the first step.

2.2. Fundamental formulae

In the frequency domain for an un-damped bounded medium, the dynamic-stiffness matrix $\boldsymbol{S}^{\mathrm{t}}(\omega)$ corresponding to all degrees of freedom is written as (superscript t for total bounded medium)

$$\boldsymbol{S}^{\mathrm{t}}(\omega) = \boldsymbol{K} - \omega^2 \boldsymbol{M} \tag{2}$$

in which $\boldsymbol{K}$ and $\boldsymbol{M}$ denote the static-stiffness matrix and mass matrix of the bounded medium with finite element respectively.

After introduce dimensionless matrix $\overline{\boldsymbol{K}}$ and $\overline{\boldsymbol{M}}$, then we have

$$\boldsymbol{K} = G r_0^{s-2} \overline{\boldsymbol{K}}, \quad \boldsymbol{M} = \rho r_0^{s} \overline{\boldsymbol{M}} \tag{3}$$

with the shear module G, mass density ρ, characteristic length r_0 and spatial dimension s ($=3$ or 2 for 3-D or 2-D problems respectively). $\overline{\boldsymbol{K}}$ does not depend on G and nor $\overline{\boldsymbol{M}}$ on ρ.

Then Eq. (2) is reformulated as

$$\boldsymbol{S}^{\mathrm{t}}(\omega) = G r_0^{s-2} (\overline{\boldsymbol{K}} - a_0^2 \overline{\boldsymbol{M}}) \tag{4}$$

where $a_0 = \omega r_0 / c_{\mathrm{s}}$ is the dimensionless frequency. $c_{\mathrm{s}} = \sqrt{G/\rho}$ is the shear-wave velocity.

After introducing artificial damping ζ, the dynamic stiffness matrix corresponding to all degrees of freedom for damped bounded medium is transformed to (subscript ζ for damping)

$$\boldsymbol{S}^{\mathrm{t}}_{\zeta}(\omega) = (1 + 2\mathrm{i}\zeta)\boldsymbol{K} - \omega^2 \boldsymbol{M} = G^* r_0^{s-2} (\overline{\boldsymbol{K}} - a_0^{*2} \overline{\boldsymbol{M}}) \tag{5}$$

in which G^* and a_0^* are the counterparts of shear module G and dimensionless frequency a_0 with artificial damping ζ respectively.

$$G^* = G(1 + 2i\zeta), \quad c_s^* = \sqrt{G^*/\rho}, \quad a_0^* = \frac{\omega r_0}{c_s^*} \tag{6}$$

Partitioning all degrees of freedom into two parts, degrees of freedom on the structure–medium interface (indicated by subscript o) and degrees of freedom not on the structure–medium interface (indicated by subscript i), Eq. (5) can be expressed in the form

$$\boldsymbol{S}_\zeta^t = \begin{bmatrix} \boldsymbol{S}_{ii} & \boldsymbol{S}_{oi} \\ \boldsymbol{S}_{io} & \boldsymbol{S}_{oo} \end{bmatrix} = (1 + 2i\zeta)\begin{bmatrix} \boldsymbol{K}_{ii} & \boldsymbol{K}_{io} \\ \boldsymbol{K}_{oi} & \boldsymbol{K}_{oo} \end{bmatrix} - \omega^2 \begin{bmatrix} \boldsymbol{M}_{ii} & \boldsymbol{M}_{io} \\ \boldsymbol{M}_{oi} & \boldsymbol{M}_{oo} \end{bmatrix} \tag{7}$$

After elimination of all degrees of freedom not located on the structure–bounded medium interface, the dynamic stiffness matrix $\boldsymbol{S}_\zeta^b(\omega)$ on the structure–bounded damped medium interface can be expressed as follows (superscript b for bounded medium–structure interface)

$$\boldsymbol{S}_\zeta^b(\omega) = \boldsymbol{S}_{oo} - \boldsymbol{S}_{oi}\boldsymbol{S}_{ii}^{-1}\boldsymbol{S}_{io} \tag{8}$$

From Eqs. (5), (7) and (8), it can be seen that the dynamic stiffness matrix $\boldsymbol{S}_\zeta^b(\omega)$ on the structure–medium interface will still be proportional to $G^* r_0^{s-2}$ and can be expressed by the corresponding dimensionless dynamic stiffness matrix $\overline{\boldsymbol{S}}^b(a_0^*)$

$$\boldsymbol{S}_\zeta^b(\omega) = G^* r_0^{s-2}\overline{\boldsymbol{S}}^b(\alpha_0^*) \tag{9}$$

Analogously there exist the relationship $\boldsymbol{S}^b(\omega) = G r_0^{s-2}\overline{\boldsymbol{S}}^b(\alpha_0)$ for the un-damped bounded medium. Together with Eqs. (4) and (5), it can be noted that $\overline{\boldsymbol{S}}^b(a_0^*)$ can be thought to be the dimensionless dynamic stiffness matrix corresponding to un-damped bounded medium at frequency a_0^*.

It is assumed that the impedance $\boldsymbol{S}_\zeta^b(\omega)$ of the damped bounded medium is approximately equal to that of the damped unbounded medium $\boldsymbol{S}_\zeta^\infty(\omega)$. The same also applies to their first derivative with respect to ω. Hence

$$\boldsymbol{S}_\zeta^\infty(\omega) = \boldsymbol{S}_\zeta^b(\omega), \quad \boldsymbol{S}_\zeta^\infty(\omega)_{,\omega} = \boldsymbol{S}_\zeta^b(\omega)_{,\omega} \tag{10}$$

Dividing Eq. (10) by $G^* r_0^{s-2}$ with

$$\boldsymbol{S}_\zeta^\infty(\omega) = G^* r_0^{s-2}\overline{\boldsymbol{S}}^\infty(a_0^*) \tag{11}$$

and with Eq. (9) yields

$$\overline{\boldsymbol{S}}^\infty(a_0^*) = \overline{\boldsymbol{S}}^b(a_0^*), \quad \overline{\boldsymbol{S}}^\infty(a_0^*)_{,\omega} = \overline{\boldsymbol{S}}^b(a_0^*)_{,\omega} \tag{12}$$

As discussed by Wolf and Song (1996), the dimensionless impedance $\overline{\boldsymbol{S}}^\infty(a_0)$ of unbounded un-damped medium is evaluated with a_0 corresponding to the same ω as a_0^*. To calculate $\overline{\boldsymbol{S}}^\infty(a_0)$, the first two terms of a Taylor expansion of $\overline{\boldsymbol{S}}^\infty(a_0^*)$ are formulated

$$\overline{\boldsymbol{S}}^\infty(a_0) = \overline{\boldsymbol{S}}^\infty(a_0^* + (a_0 - a_0^*)) = \overline{\boldsymbol{S}}^\infty(a_0^*) + \overline{\boldsymbol{S}}^\infty(a_0^*)_{,a_0^*}(a_0 - a_0^*) \tag{13}$$

Using Eqs. (9) and (12) with

$$\boldsymbol{S}^\infty(\omega) = G r_0^{s-2}\overline{\boldsymbol{S}}^\infty(a_0) \tag{14}$$

and multiplying the right hand of Eq. (13) by $G^* r_0^{s-2}$ to converse the dimensionless impedance matrix to actual impedance matrix yields

$$\boldsymbol{S}^\infty(\omega) = \frac{G}{G^*}\left(\boldsymbol{S}_\zeta^b(\omega) + \boldsymbol{S}_\zeta^b(\omega)_{,\omega}\frac{a_0 - a_0^*}{a_{0,\omega}^*}\right) \tag{15}$$

Substituting $(a_0 - a_0^*)/a_{0,\omega}^* = \omega\left(\sqrt{1+2i\zeta}-1\right)$ into above equation leads to

$$\boldsymbol{S}^{\infty}(\omega) = \frac{1}{1+2i\zeta}\left(\boldsymbol{S}_{\zeta}^{b}(\omega) + \left(\sqrt{1+2i\zeta}-1\right)\omega\boldsymbol{S}_{\zeta}^{b}(\omega)_{,\omega}\right) \tag{16}$$

Wolf and Song (1996) propose such algorithm for matrix $\boldsymbol{S}^{\infty}(\omega)$ as

$$\boldsymbol{S}^{\infty}(\omega_j) = \frac{1}{1+2i\zeta}\left(\boldsymbol{S}_{\zeta}^{b}(\omega_j) + \left(\sqrt{1+2i\zeta}-1\right)\omega_j\boldsymbol{S}_{\zeta}^{b}(\omega_j)_{,\omega|\omega=\omega_j}\right) \tag{17}$$

$$\boldsymbol{S}_{\zeta}^{b}(\omega_j)_{,\omega|\omega=\omega_j} = \frac{\boldsymbol{S}_{\zeta}^{b}(\omega_{j+1}) - \boldsymbol{S}_{\zeta}^{b}(\omega_{j-1})}{\omega_{j+1}-\omega_{j-1}} \tag{18}$$

which needs three times computational cost of Eq. (8) in first step for a given frequency ω_j.

3. Recursive procedure for impedance of unbounded medium

The efficiency of the solving Eqs. (8) and (18) is of great significance because they have to be repeated for a series of frequencies. Thus the algorithm, which consists of three steps, is focused on the efficiency of the solving of $\boldsymbol{S}_{ii}^{-1}\boldsymbol{S}_{io}$ in Eq. (8) and $\boldsymbol{S}_{\zeta}^{b}(\omega)_{,\omega}$ in Eq. (18).

3.1. Accurate formulae for $\boldsymbol{S}_{\zeta}^{b}(\omega)_{,\omega}$

The use of Eq. (18) is not an efficient procedure for $\boldsymbol{S}_{\zeta}^{b}(\omega)_{,\omega}$. In this step, an accurate formula for $\boldsymbol{S}_{\zeta}^{b}(\omega)_{,\omega}$ is derived to reduce the computational cost of Eq. (18).

First, for specified frequency ω_j, some notations are set for conciseness as follows (see Eq. (8))

$$\Delta\omega = \omega_{j+1} - \omega_j \tag{19a}$$

$$\boldsymbol{S}_j = \boldsymbol{S}_{ii}(\omega_j), \quad \boldsymbol{S}_{j+1} = \boldsymbol{S}_{ii}(\omega_{j+1}) \tag{19b}$$

$$\boldsymbol{Y}_j = \boldsymbol{S}_{ii}^{-1}(\omega_j)\boldsymbol{S}_{io} = \boldsymbol{S}_j^{-1}\boldsymbol{S}_{io},\ \boldsymbol{Y}_{j+1} = \boldsymbol{S}_{ii}^{-1}(\omega_{j+1})\boldsymbol{S}_{io} = \boldsymbol{S}_{j+1}^{-1}\boldsymbol{S}_{io} \tag{19c}$$

For the sake of simplicity a lumped-mass matrix of the finite element is chosen, then the off-diagonal terms of the matrix $\boldsymbol{S}_{io}$ equal $\boldsymbol{S}_{oi}^{T}$ and do not vary with frequency as shown in Eq. (7).

By virtues of Eqs. (7) and (19b), we obtain

$$\boldsymbol{S}_j = (1+2i\zeta)\boldsymbol{K}_{ii} - \omega_j^2\boldsymbol{M}_{ii} \tag{20}$$

$$\boldsymbol{S}_{j+1} = (1+2i\zeta)\boldsymbol{K}_{ii} - (\omega_j+\Delta\omega)^2\boldsymbol{M}_{ii} = \boldsymbol{S}_j - h_j\boldsymbol{M}_{ii} \tag{21}$$

in which

$$h_j = h(\omega_j, \Delta\omega) = 2\omega_j\Delta\omega + \Delta\omega^2 \quad \text{for } \omega_{j+1} = \omega_j + \Delta\omega \tag{22}$$

Defining

$$\boldsymbol{S}_{j+1} = \boldsymbol{S}_j + \Delta\boldsymbol{S}_{j+1}, \quad \boldsymbol{Y}_{j+1} = \boldsymbol{Y}_j + \Delta\boldsymbol{Y}_{j+1} \tag{23}$$

and using Eq. (21), we can obtain

$$\Delta\boldsymbol{S}_{j+1} = -h_j \cdot \boldsymbol{M}_{ii} \tag{24}$$

Using the following relationships based on Eqs. (19c) and (23)

$$\boldsymbol{S}_{\mathrm{io}} = \boldsymbol{S}_j \boldsymbol{Y}_j = \boldsymbol{S}_{j+1} \boldsymbol{Y}_{j+1} = (\boldsymbol{S}_j + \Delta \boldsymbol{S}_{j+1})(\boldsymbol{Y}_j + \Delta \boldsymbol{Y}_{j+1}) \tag{25}$$

we can get

$$\Delta \boldsymbol{Y}_{j+1} = -\boldsymbol{S}_j^{-1} \Delta \boldsymbol{S}_{j+1} (\boldsymbol{Y}_j + \Delta \boldsymbol{Y}_{j+1}) \tag{26}$$

An iterative procedure for $\Delta \boldsymbol{Y}_{j+1}$ can be formulated from Eq. (26) as

$$\Delta \boldsymbol{Y}_{j+1}^{k+1} = -\boldsymbol{S}_j^{-1} \Delta \boldsymbol{S}_{j+1} (\boldsymbol{Y}_j + \Delta \boldsymbol{Y}_{j+1}^{k}) \tag{27}$$

Using Eq. (24), above equation can be further expressed as

$$\Delta \boldsymbol{Y}_{j+1}^{k+1} = h_j \boldsymbol{S}_j^{-1} \boldsymbol{M}_{\mathrm{ii}} (\boldsymbol{Y}_j + \Delta \boldsymbol{Y}_{j+1}^{k}) = h_j \boldsymbol{X}_j (\boldsymbol{Y}_j + \Delta \boldsymbol{Y}_{j+1}^{k}) \tag{28}$$

where

$$\boldsymbol{X}_j = \boldsymbol{S}_j^{-1} \boldsymbol{M}_{\mathrm{ii}} \tag{29}$$

Since $\boldsymbol{S}_j$ and $\boldsymbol{M}_{\mathrm{ii}}$ are symmetric, $\boldsymbol{X}_j = \boldsymbol{X}_j^{\mathrm{T}}$ applies.

Eq. (28) can be further expressed in series form as

$$\Delta \boldsymbol{Y}_{j+1} = h_j \boldsymbol{X}_j (\boldsymbol{I} + (h_j \boldsymbol{X}_j) + (h_j \boldsymbol{X}_j)^2 + \cdots) \boldsymbol{Y}_j \tag{30}$$

in which $\boldsymbol{I}$ is unit matrix.

The derivative of $\boldsymbol{S}_{\zeta}^{\mathrm{b}}(\omega)$ with respect to ω is written as

$$\boldsymbol{S}_{\zeta}^{\mathrm{b}}(\omega_j)_{,\omega} = \lim_{\Delta\omega \to 0} \frac{\boldsymbol{S}_{\zeta}^{\mathrm{b}}(\omega_j + \Delta\omega) - \boldsymbol{S}_{\zeta}^{\mathrm{b}}(\omega_j)}{\Delta\omega} \tag{31}$$

By virtues of Eqs. (8), (19c) and (23), Eq. (31) is expressed as

$$\boldsymbol{S}_{\zeta}^{\mathrm{b}}(\omega_j)_{,\omega} = \lim_{\Delta\omega \to 0} \frac{\boldsymbol{S}_{\mathrm{oo}}(\omega_j + \Delta\omega) - \boldsymbol{S}_{\mathrm{oo}}(\omega_j)}{\Delta\omega} - \lim_{\Delta\omega \to 0} \frac{\boldsymbol{S}_{\mathrm{oi}}(\boldsymbol{Y}_{j+1} - \boldsymbol{Y}_j)}{\Delta\omega} = \boldsymbol{S}_{\mathrm{oo},\omega} - \lim_{\Delta\omega \to 0} \frac{\boldsymbol{S}_{\mathrm{oi}} \Delta \boldsymbol{Y}_{j+1}}{\Delta\omega} \tag{32}$$

Substituting Eqs. (7) and (30) into Eq. (32), the derivative of $\boldsymbol{S}_{\zeta}^{\mathrm{b}}(\omega_j)$ with respect to frequency can be given as

$$\boldsymbol{S}_{\zeta}^{\mathrm{b}}(\omega_j)_{,\omega} = -2\omega_j \boldsymbol{M}_{\mathrm{oo}} - \lim_{\Delta\omega \to 0} \boldsymbol{S}_{\mathrm{oi}} \boldsymbol{X}_j \frac{h_j(\boldsymbol{I} + (h_j \boldsymbol{X}_j) + \cdots)}{\Delta\omega} \boldsymbol{Y}_j = -2\omega_j \boldsymbol{M}_{\mathrm{oo}} - 2\omega_j \boldsymbol{S}_{\mathrm{oi}} \boldsymbol{X}_j \boldsymbol{Y}_j$$

Together with Eqs. (29) and (19c), the accurate formula for derivative of $\boldsymbol{S}_{\zeta}^{\mathrm{b}}(\omega_j)$ is as follows

$$\boldsymbol{S}_{\zeta}^{\mathrm{b}}(\omega_j)_{,\omega} = -2\omega_j (\boldsymbol{M}_{\mathrm{oo}} + \boldsymbol{Y}_j^{\mathrm{T}} \boldsymbol{M}_{\mathrm{ii}} \boldsymbol{Y}_j) \tag{33}$$

which leads to the dynamic stiffness matrix of unbounded medium as

$$\boldsymbol{S}^{\infty}(\omega_j) = \frac{1}{1 + 2\mathrm{i}\zeta} \left(\boldsymbol{S}_{\mathrm{oo}} - \boldsymbol{S}_{\mathrm{io}} \boldsymbol{Y}_j - 2\left(\sqrt{1 + 2\mathrm{i}\zeta} - 1 \right) \omega_j^2 (\boldsymbol{M}_{\mathrm{oo}} + \boldsymbol{Y}_j^{\mathrm{T}} \boldsymbol{M}_{\mathrm{ii}} \boldsymbol{Y}_j) \right) \tag{34}$$

Intermediate matrix $\boldsymbol{Y}_j = \boldsymbol{S}_j^{-1}(\omega_j) \boldsymbol{S}_{\mathrm{io}}$ is utilized to obtain $\boldsymbol{S}_{\zeta}^{\mathrm{b}}(\omega_j)$ and its derivative, which leads to a drastic reduction of the computational cost to only 1/3 of that by Eq. (18) for a specified frequency of interested.

3.2. Iterative procedure for the dynamic stiffness matrices for a series of frequencies

It can be seen from Eqs. (8) and (19c) that solving $\boldsymbol{Y}_j = \boldsymbol{S}_j^{-1}(\omega_j) \boldsymbol{S}_{\mathrm{io}}$ contributes most of the computational cost to the determination of the impedance on structure–medium interface. If for ω_{j+1}, $\boldsymbol{Y}_{j+1}$ can be

obtained from Eqs. (23) and (28) instead of from Eqs. (8) or (18), the computational cost can be further reduced.

The orders of magnitude o of the property matrices are $\boldsymbol{K} = \mathrm{o}(Gr_0^{s-2})$ and $\boldsymbol{M} = \mathrm{o}(\rho r_0^s)$.

Defining

$$\boldsymbol{X}_j = -\boldsymbol{S}_j^{-1}\boldsymbol{M}_{\mathrm{ii}}, \quad \boldsymbol{X}_{j+1} = -\boldsymbol{S}_{j+1}^{-1}\boldsymbol{M}_{\mathrm{ii}} \tag{35}$$

then it follows from Eq. (18) and above expression that $\boldsymbol{Y}_j = \mathrm{o}(1)$, $\boldsymbol{X}_j = \mathrm{o}(\rho r^2/G)$.

Defining the power series in Eq. (18) as transfer matrix

$$\boldsymbol{A}_j = \boldsymbol{I} + (h_j\boldsymbol{X}_j) + (h_j\boldsymbol{X}_j)^2 + \cdots \tag{36}$$

which has the property of $\boldsymbol{A}_j = \boldsymbol{I} + (h_j\boldsymbol{X}) \cdot \boldsymbol{A}_j$ then Eq. (28) can be further expressed

$$\Delta\boldsymbol{Y}_{j+1} = h_j\boldsymbol{X}_j\boldsymbol{A}_j\boldsymbol{Y}_j \tag{37}$$

Using Eq. (23), $\boldsymbol{Y}_{j+1}$ at ω_{j+1} can be obtained from $\boldsymbol{Y}_j$ at ω_j by multiplying transfer matrix $\boldsymbol{A}_j$

$$\boldsymbol{Y}_{j+1} = (\boldsymbol{I} + (h_j\boldsymbol{X}_j)\boldsymbol{A}_j)\boldsymbol{Y}_j = \boldsymbol{A}_j\boldsymbol{Y}_j \tag{38}$$

The large underground hydroelectric power plants like Xi Luodu project are usually located at rock region with shear modulus G of magnitude $\mathrm{o}(10^{10})$ (Pa), mass density ρ of magnitude of $\mathrm{o}(10^3)$ (kg/m^3) and characteristic length r of $\mathrm{o}(10^1)$ (m), so $\boldsymbol{X}_j$ has the order of magnitude $\mathrm{o}(10^{-5})$ (see Eqs. (7) and (35); In engineering seismic analysis, the frequencies of interested are usually in the range of $(0, 10^2)$, then we have $h_j = \mathrm{o}(10)$ if $\Delta\omega$ is set comparatively small as $\mathrm{o}(10^{-1})$.

So, only the first three terms in the bracket of Eq. (36) can give satisfactory results with relative error tolerance of magnitude $\mathrm{o}(10^{-10})$ for $\boldsymbol{Y}_{j+1}$, That is

$$\boldsymbol{A}_j = \boldsymbol{I} + (h_j\boldsymbol{X}_j) + (h_j\boldsymbol{X}_j)^2 \tag{39}$$

Thus $\boldsymbol{Y}_{j+1}$ can be obtained from the matrix $\boldsymbol{Y}_j$ and $\boldsymbol{X}_j$ at frequency ω_j based on Eq. (38) instead of Eq. (19c) which would takes great computational effort. Then from Eq. (34), the impedance matrix $\boldsymbol{S}^{\infty}(\omega_j)$ at frequency ω_{j+1} can be obtained from $\boldsymbol{Y}_{j+1}$.

But the computational costs are still great if $\boldsymbol{X}_{j+1}$ is gotten from Eq. (35) for frequency ω_{j+1}, so the analogous recursive procedure for the computation of $\boldsymbol{X}_{j+1}$ is derived.

Assume

$$\boldsymbol{X}_{j+1} = \boldsymbol{X}_j + \Delta\boldsymbol{X}_{j+1} \tag{40}$$

Then from Eqs. (23) and (35), we have

$$\boldsymbol{M}_{\mathrm{ii}} = \boldsymbol{S}_j\boldsymbol{X}_j = \boldsymbol{S}_{j+1}\boldsymbol{X}_{j+1} = (\boldsymbol{S}_j + \Delta\boldsymbol{S}_{j+1}) \cdot (\boldsymbol{X}_j + \Delta\boldsymbol{X}_j) \tag{41}$$

which leads to

$$\Delta\boldsymbol{X}_{j+1} = h_j\boldsymbol{X}_j(\boldsymbol{X}_j + \Delta\boldsymbol{X}_{j+1}) \tag{42}$$

Analogous to the derivation for $\boldsymbol{Y}_{j+1}$, the recursive procedure about $\boldsymbol{X}_{j+1}$ can be written in the following forms as

$$\Delta\boldsymbol{X}_{j+1}^{k+1} = h_j\boldsymbol{X}_j(\boldsymbol{X}_j + \Delta\boldsymbol{X}_{j+1}^{k}) \tag{43}$$

$$\Delta\boldsymbol{X}_{j+1} = h_j\boldsymbol{X}_j(\boldsymbol{I} + (h_j\boldsymbol{X}_j) + (h_j\boldsymbol{X}_j)^2 + \cdots)\boldsymbol{X}_j = h_j\boldsymbol{X}_j\boldsymbol{A}_j\boldsymbol{X}_j \tag{44}$$

and

$$\boldsymbol{X}_{j+1} = \boldsymbol{A}_j\boldsymbol{X}_j \tag{45}$$

Eq. (45) takes the same form to Eq. (38).

Obtaining $\boldsymbol{X}_{j+1}$ from Eq. (45) can avoid the solving of Eq. (35) and would greatly reduce the computational cost for a series of frequencies.

3.3. Summary of procedure

The procedure for the impedance matrix $\boldsymbol{S}^{\infty}(\omega_j)$ of unbounded medium developed in the preceding sections may be summarized as follows.

Initialization (for a given starting frequency)

$$\boldsymbol{S}_{\mathrm{ii}}(\omega_0) = (1+2\mathrm{i}\zeta)\boldsymbol{K}_{\mathrm{ii}} - \omega_0^2\boldsymbol{M}_{\mathrm{ii}}, \quad \boldsymbol{S}_{\mathrm{oo}}(\omega_0) = (1+2\mathrm{i}\zeta)\boldsymbol{K}_{\mathrm{oo}} - \omega_0^2\boldsymbol{M}_{\mathrm{oo}}$$

$$\boldsymbol{S}_{\mathrm{io}} = \boldsymbol{S}_{\mathrm{oi}}^{\mathrm{T}} = (1+2\mathrm{i}\zeta)\boldsymbol{K}_{\mathrm{io}}$$

$$\boldsymbol{X}_0 = -\boldsymbol{S}_{\mathrm{ii}}^{-1}(\omega_0)\boldsymbol{M}_{\mathrm{ii}}, \quad \boldsymbol{Y}_0 = \boldsymbol{S}_{\mathrm{ii}}^{-1}(\omega_0)\boldsymbol{S}_{\mathrm{io}}$$

$$\boldsymbol{S}^{\infty}(\omega_0) = \frac{1}{1+2\mathrm{i}\zeta}\left(\boldsymbol{S}_{\mathrm{oo}}(\omega_0) - \boldsymbol{S}_{\mathrm{io}}\boldsymbol{Y}_0 - 2\left(\sqrt{1+2\mathrm{i}\zeta}-1\right)\omega_0^2(\boldsymbol{M}_{\mathrm{oo}} + \boldsymbol{Y}_0^{\mathrm{T}}\boldsymbol{M}_{\mathrm{ii}}\boldsymbol{Y}_0)\right)$$

Recursive procedure

For $j = 0, n$

$$\omega_{j+1} = \omega_j + \Delta\omega$$

$$h_j = h(\omega_j, \Delta\omega) = 2\omega_j\Delta\omega + \Delta\omega^2$$

$$\boldsymbol{S}_{\mathrm{oo}}(\omega_{j+1}) = (1+2\mathrm{i}\zeta)\boldsymbol{K}_{\mathrm{oo}} - \omega_{j+1}^2\boldsymbol{M}_{\mathrm{oo}}$$

$$\boldsymbol{A}_j = \boldsymbol{I} + (h_j\boldsymbol{X}_j) + (h_j\boldsymbol{X}_j)^2 + \cdots \quad \text{or} \quad \boldsymbol{A}_j = \boldsymbol{I} + (h_j\boldsymbol{X}_j) + (h_j\boldsymbol{X}_j)^2$$

$$\boldsymbol{X}_{j+1} = \boldsymbol{A}_j\boldsymbol{X}_j, \quad \boldsymbol{Y}_{j+1} = \boldsymbol{A}_j\boldsymbol{Y}_j$$

$$\boldsymbol{S}^{\infty}(\omega_{j+1}) = \frac{1}{1+2\mathrm{i}\zeta}\left(\boldsymbol{S}_{\mathrm{oo}}(\omega_{j+1}) - \boldsymbol{S}_{\mathrm{io}}\boldsymbol{Y}_{j+1} - 2\left(\sqrt{1+2\mathrm{i}\zeta}-1\right)\omega_{j+1}^2(\boldsymbol{M}_{\mathrm{oo}} + \boldsymbol{Y}_{j+1}^{\mathrm{T}}\boldsymbol{M}_{\mathrm{ii}}\boldsymbol{Y}_{j+1})\right)$$

4. Seismic response analysis of Xiluodu hydropower plant

Several examples, which had been discussed by Wolf and Song (1996), are examined here to illustrate the accuracy and effectiveness of the proposed method, then the procedure is applied to the impedance computation of the unbounded rock medium in which located Xiluodu underground power plant. Incorporated with the substructure method, the dynamic response of underground caverns-unbounded rock medium interaction system to earthquake excitation is analyzed.

4.1. Semi-infinite rod on elastic foundation

A semi-infinite rod on elastic foundation, illustrated in Fig. 1, is used to demonstrate accuracy of the proposed method for simulating one-dimensional wave propagation problem. As will become apparent, this is a dispersive system, i.e. the phase velocity is a function of frequency. In addition, a so-called cut-off

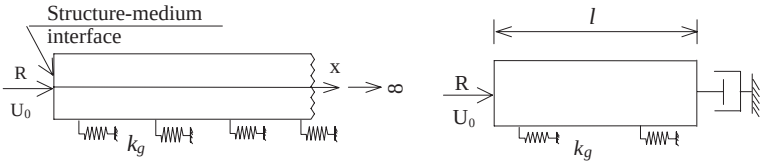

Fig. 1. Semi-infinite rod on elastic foundation.

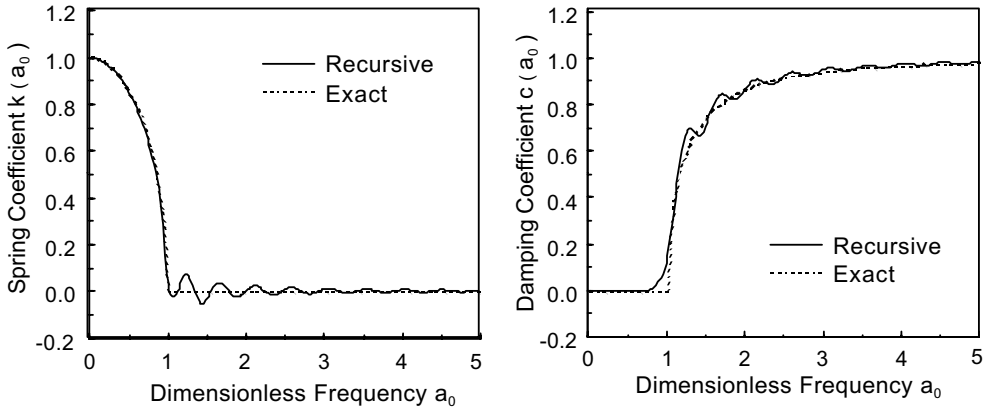

Fig. 2. Dynamic-stiffness coefficient of semi-infinite rod on elastic foundation.

frequency occurs below which no waves propagate. With an analytical solution available given by Wolf and Song (1996), it is thus a stringent test.

In the finite region adjacent to the structure–unbounded medium interface, artificial damping $\zeta = 0.1$ is introduced. The area of the rod is denoted by A, the modulus of elasticity by E, the mass density by ρ, and the static spring stiffness per unit length of the elastic foundation by k_g, at the outer boundary a viscous dashpot is introduced to further reduce the length l of bounded medium.

The normalized results (solid line) are plotted in Fig. 2, in which $r_0 = \sqrt{EA/k_g}$, $c_l = \sqrt{E/\rho}$, $a_0 = \omega r_0/c_l$ and $l/r_0 = 4$. As can be seen from the comparison with the analytical solution (dashed line), the agreement is excellent.

4.2. Out-of-plane motion of semi-infinite layer

As a two-dimensional wave propagation problem with an analytical solution available, the out-of-plane motion of a semi-infinite layer of constant depth d shown in Fig. 3 is addressed. Out of the boundaries

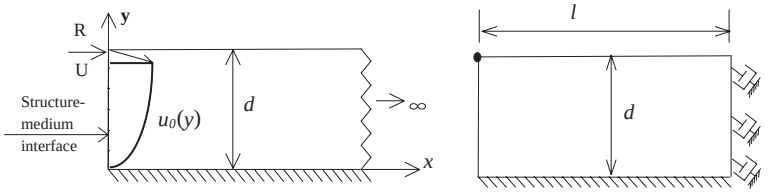

Fig. 3. Out-of-plane motion of semi-infinite layer with prescribed displacement.

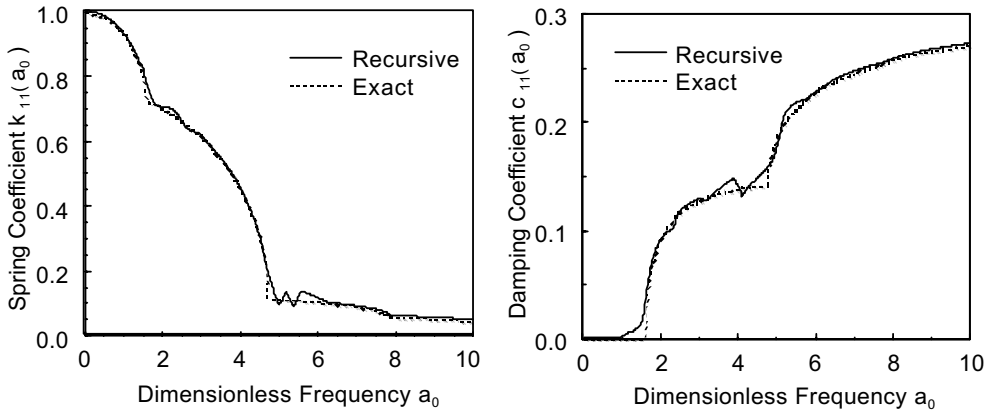

Fig. 4. Diagonal term of corner node in dynamic-stiffness matrix of semi-infinite layer.

extending to infinity in the radial direction is fixed and the other is a free surface. The structure–medium interface coincides with the y-axis.

The material behavior of the homogeneous layer is characterized by the shear module G and mass density ρ. The dynamic-stiffness matrix at the structure–medium interface corresponding to a parabolic variation of the displacement $u_0(y)$ is calculated. As will become apparent, this system has a cut-off frequency at the layer's fundamental natural frequency. At this frequency and at each of the higher natural frequencies, a Love mode starts with a phase velocity of infinity, which decreases for higher frequencies, converging to the shear-wave velocity for infinite frequency, this case, which often occurs in practice, is thus a very stringent test.

The dimensionless spring and damping coefficients (solid line) are plotted versus a_0 in Fig. 4, in which, $c_s = \sqrt{G/\rho}$, $a_0 = \omega d/c_s$. The analytical results (Wolf and Song, 1996) are also plotted in dashed line for comparison and it proves the good accuracy of the method.

4.3. Out-of-plane motion of semi-infinite wedge

As another two-dimensional wave propagation problem shown in Fig. 5, a semi-infinite wedge with an opening angle α and with a free and a fixed boundary extending to infinity in the radial direction is investigated to further verify the proposed method. The example describes an out-of-plane motion governed by the scalar wave equation.

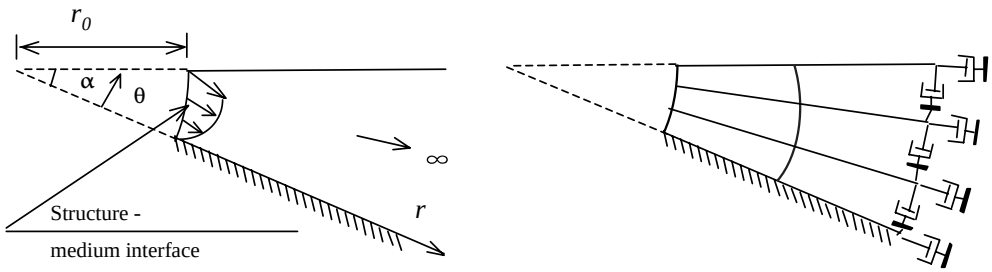

Fig. 5. Out-of-plane motion of semi-infinite wedge with prescribed displacement.

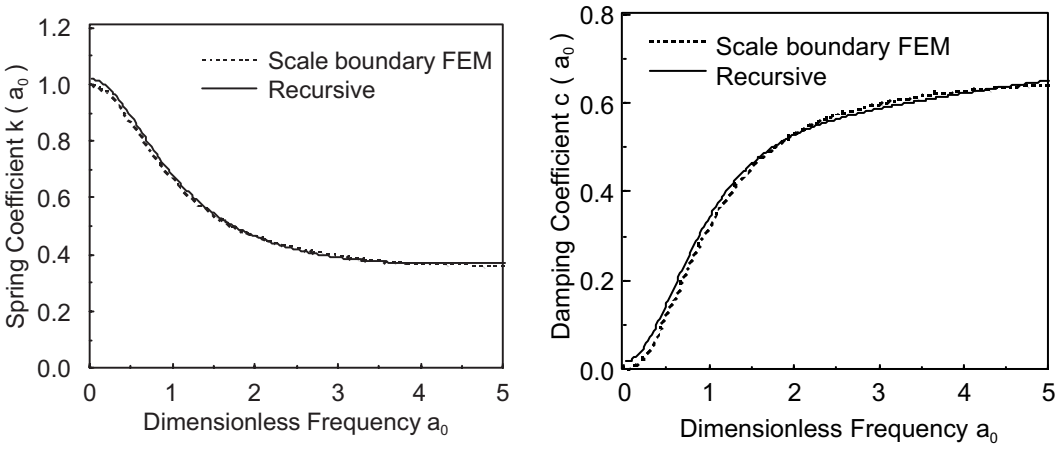

Fig. 6. Dynamic-stiffness coefficient of semi-infinite wedge.

The typical constants of the semi-infinite wedge are the shear modulus G and the mass density ρ, the structure–medium interface coincides with the arc determined by the radius r_0, where the motion as a linear function of the angle is prescribed. The same problem is also computed by scaled boundary finite-element method for comparison shown in Fig. 6, which can be seen as exact solution.

This example shows that the proposed method can give very satisfactory result.

4.4. Seismic response of Xiluodu large underground power plant

The accuracy of the proposed method has been verified by the above numerical results and the computational time is reduced greatly compared with the original procedure (Wolf and Song, 1996). And now the recursive procedure is applied to the seismic analysis of Xiluodu underground power plant caverns.

Xiluodu arch dam is one of the several huge hydropower projects being building or will be built in seismic active south-west China. The underground power plant cavern is about 448 m long, 74.4 m high and 30 m wide.

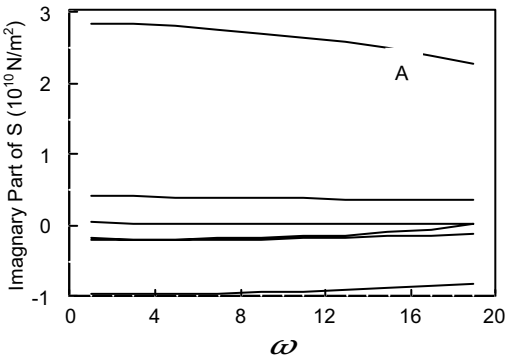

Fig. 7. Real part variation with frequency of wall rock dynamic impedance.

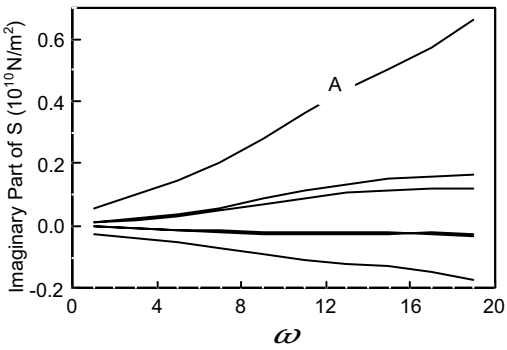

Fig. 8. Imaginary part variation with frequency of wall rock dynamic impedance.

The variation of the dynamic stiffness of unbounded rock medium in Xiluodu zone with frequency is demonstrated in Figs. 7 and 8, in which the lines marked with A denote diagonal terms of the impedance matrix, others denote off-diagonal terms.

From Figs. 7 and 8, it can be shown that the real and imaginary part of the impedance vary with frequency slowly in the engineering interested frequency range.

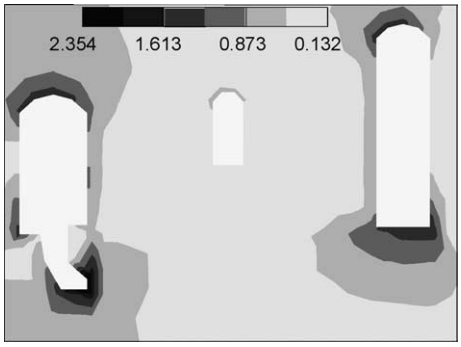

Fig. 9. Maximum main stress distribution of underground group caverns (unit: MPa).

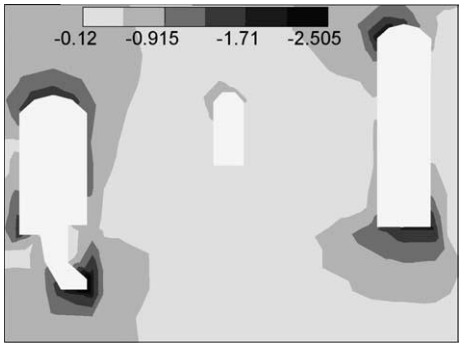

Fig. 10. Minimal main stress distribution of underground group caverns (unit: MPa).

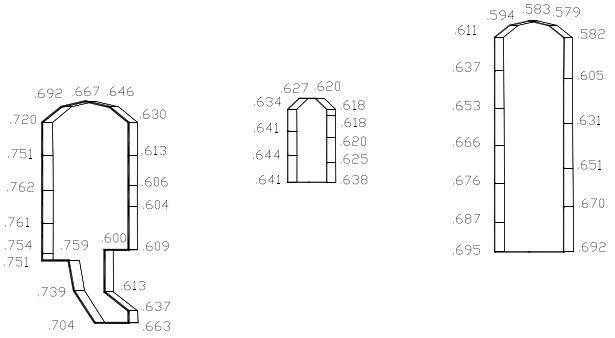

Fig. 11. Maximum displacement distribution of underground group caverns (unit: cm).

The underground hydropower plant includes several caverns, which are used for electricity generation, electric transforming equipment, and two wells for adjusting hydraulic pressure.

Rock material is linear orthotropic with lateral modulus 2.0×10^{10} Pa, vertical modulus 1.5×10^{10} Pa, Poisson's ratio 0.2, mass density 2850 kg/m^3. The concrete linings of the cavern are linear isotropic material with elastic modulus 3.0×10^{10} Pa, Poisson's ratio 0.17, mass density 2400 kg/m^3. A seismic wave recorded on rock at San Fernando in 1971 is selected.

The maximum and minimal response results of one representative cross section through the time history are shown in Figs. 9–11.

From Figs. 9 and 10, it is demonstrated that the response of middle cavern is very small compared with that of side caverns because of the shielding effect of side cavern to seismic wave.

5. Conclusion

A high performance recursive damping-solvent method is presented. The method in conjunction with substructure method for the seismic analysis of large underground caverns can results in a great reduction of computational costs with high accuracy and efficiency. It can be used as the appropriate tool for the dynamic analysis of various underground structures.

Acknowledgements

This work was carried out with the support of the National Nature Science Foundation of China; under contract/grant agreement number: 50209002 and the support of the Liaoning Province Science and Technology Foundation (grant number 20022130). The authors wish to thank Dr. J.P Wolf and Dr. C.M. Song for providing the program about Consistent Infinitesimal Finite-Element Cell method.

References

Chow, Y.K., Smith, I.M., 1981. Static and periodic infinite solid elements. International Journal for Numerical Methods in Engineering 17, 503–526.

Dasgupta, G., 1982. A finite element formulation for unbounded homogeneous continua. ASCE Journal of Applied Mechanics 49, 136–140.

Stamos, A.A., Beskos, D.E., 1995. Dynamic analysis of large 3-d underground structures by the BEM. Earthquake Engineering and Structure Dynamics 24, 917–934.

Werkle, H., 1987. A transmitting boundary for the dynamic finite element analysis of cross anisotropic soils. Earthquake Engineering and Structure Dynamics 15, 831–838.

Wolf, J.P., Motosaka, M., 1989. Recursive evaluation of interaction forces of unbounded soil in the time domain. Earthquake Engineering and Structure Dynamics 18, 345–363.

Wolf, J.P., Song, C., 1994a. Dynamic stiffness matrix in time domain of unbounded medium by infinitesimal finite element cell method. Earthquake Engineering and Structure Dynamics 23, 1181–1198.

Wolf, J.P., Song, C., 1994b. Dynamic stiffness matrix of unbounded soil by finite element multi-cell cloning method. Earthquake Engineering and Structure Dynamics 23, 233–250.

Wolf, J.P., Song, C., 1995. Consistent infinitesimal finite element cell method: in-plane motion. Computer Methods in Applied Mechanics Engineering 123, 355–370.

Wolf, J.P., Song, C., 1996. Finite Element Model for Infinite Media. John Wiley & Sons Ltd., England.

Zhao, C., Valliappan, S., 1993. A dynamic infinite element for three-dimensional infinite domain wave problems. International Journal for Numerical Methods in Engineering 36, 2567–2580.